

## Precise predictions for LHC using a GOLEM

T. Binoth<sup>a\*</sup>, A. Guffanti<sup>b</sup>, J.-Ph. Guillet<sup>c</sup>, G. Heinrich<sup>d</sup>, S. Karg<sup>e</sup>, N. Kauer<sup>f</sup>, P. Mertsch<sup>g</sup>, T. Reiter<sup>a</sup>, J. Reuter<sup>b</sup>, and G. Sanguinetti<sup>c</sup>

<sup>a</sup>School of Physics, The University of Edinburgh, Edinburgh EH9 3JZ, UK

<sup>b</sup>Department of Physics, University of Freiburg, Hermann-Herder-Str. 3a, D-79104 Freiburg, Germany

<sup>c</sup>LAPTH, 9, Chemin de Bellevue BP 110, 74941 Annecy le Vieux, France

<sup>d</sup>IPPP, University of Durham, Durham DH1 3LE, UK

<sup>e</sup>Institute for Theoretical Physics E, RWTH Aachen, D-52056 Aachen, Germany

<sup>f</sup>Institute for Theoretical Physics, University of Würzburg, D-97074 Würzburg, Germany

<sup>g</sup>Rudolf Peierls Centre for Theoretical Physics, University of Oxford, 1Keble Road, Oxford, OX1 3NP, UK

Edinburgh 2008/24, IPPP/08/49, DCPT/08/98, LAPTH/CONF-1260/08, PITHA 08/17

In this talk we present recent next-to-leading order results relevant for LHC phenomenology obtained with the GOLEM method. After reviewing the status of this Feynman diagrammatic approach for multi-leg one-loop calculations we discuss three applications: the loop-induced process  $gg \rightarrow Z^* Z^*$  and the virtual corrections to the five and six point processes  $qq \rightarrow ZZg$  and  $u\bar{u} \rightarrow s\bar{c}c$ . We demonstrate that our method leads to representations of such amplitudes which allow for efficient phase space integration. In this context we propose a reweighting technique of the leading order unweighted events by local K-factors.

### 1. Introduction

The Large Hadron Collider will explore our understanding of fundamental interactions in the multi-TeV range. Apart from testing the Higgs mechanism which is the final cornerstone of the Standard Model (SM), also a plethora of extensions of the SM will be put under scrutiny. Whatever final states will be detected, the initial state will always consist of QCD partons. The perturbative description of such processes is necessarily plagued by renormalisation and factorisation scale uncertainties. Only if next-to-leading order (NLO) corrections are included the logarithmic dependence on these scales is tamed and one ar-

rives at sufficiently reliable predictions for various signal and background processes. For a discussion of what remains to be done see [1].

For a full next-to-leading order evaluation of an N-point process one has to combine virtual corrections with real-emission corrections using some infrared subtraction method. The tree-like processes can be evaluated by using standard leading order tools. Meanwhile, automated ways to deal with the IR subtractions based on the Catani-Seymour dipole approach [2] are also on the market [3,4]. The evaluation of the one-loop contribution for N-point processes is not yet at this level of automation, although new ideas emerged and a lot of progress has been made recently in various directions [5,6,7,8,9,10,11,12].

\*This work was supported by the British Science and Technology Facilities Council (STFC) and the Scottish Universities Physics Alliance (SUPA).

## 2. The GOLEM method

The aim of our collaboration is to provide a tool which allows for a numerically stable evaluation of multi-leg one-loop amplitudes: `GOLEM`<sup>2</sup>. It is based on the method described in [13,14]. The approach relies on the evaluation of Feynman diagrams and the reduction of tensor integrals using a form factor approach. The form factors can be evaluated in various ways as outlined below.

We organize the evaluation of a one-loop amplitude as follows:

- generate Feynman diagrams using `QGRAF` [15] or `FeynArts 3.2` [17].
- separate and perform colour algebra
- project on helicity amplitudes

At this point two independent set-ups exist. Firstly, a completely symbolic reduction to standard scalar integrals with up to four external legs can be obtained using `FORM` [16] and `MAPLE`.

$$\mathcal{M}^{\{\lambda\}} \rightarrow C_{box} I_4^{n+2} + C_{tri} I_3^n + C_{bub} I_2^n + C_{tad} I_1^n + \mathcal{R}.$$

The respective coefficients are rational polynomials in Mandelstam variables. The extraction of the rational part,  $\mathcal{R}$ , of the amplitude can be done separately [18]. As long as no efficient tools for the manipulation of multivariate rational polynomials are available, interactive user input is needed to produce sufficiently compact amplitude expressions in the purely symbolic approach. Secondly, apart from the symbolic approach, we provide a numerical tensor reduction. Schematically the amplitude is expressed in terms of form factors which resemble Feynman parameter integrals with Feynman parameters in the numerator.

$$\mathcal{M}^{\{\lambda\}} \rightarrow C_{box}^{ijk} I_4^{n+2,n+4}(x_i x_j x_k) + C_{tri}^{ijk} I_3^{n,n+2}(x_i x_j x_k) + \dots$$

These form factors are implemented in a `FORTAN90` code and can be evaluated by numerical reduction and also by using one-dimensional integral representations. The form factors were designed to avoid the occurrence of so-called Gram

determinants which usually hamper a numerically stable evaluation of large Feynman diagrammatic expressions. Our method has been successfully applied to various calculations with up to six point functions [19,20,21,22].

## 3. Applications for LHC phenomenology

We discuss now recent evaluations of three loop amplitudes which are relevant in the context of Higgs searches at the LHC.

### 3.1. The process $gg \rightarrow Z^* Z^*$

In [23,24,25] it has been shown that the gluon induced production of charged vector boson pairs accounts for about 30 percent of the background to Higgs searches in that channel after cuts. Although a similar calculation for neutral vector bosons has been performed a long time ago [26], no public code is available which motivated us to redo this calculation using our method.

As only 4-point functions are present, a symbolic expression for the amplitude could be obtained, where numerically dangerous denominators have been cancelled algebraically. The expressions are implemented in a flexible computer program `GGZZ` [27] which also contains the photonic contributions. The size of the gluon contribution to the  $ZZ$  cross section in relation to the quark induced part is included in the following table:

$\sigma(pp \rightarrow Z^*(\gamma^*)Z^*(\gamma^*) \rightarrow \ell\bar{\ell}\ell'\bar{\ell}')$ [fb]					
$gg$		$q\bar{q}$		$\frac{\sigma_{\text{NLO}}}{\sigma_{\text{LO}}}$	$\frac{\sigma_{\text{NLO}+gg}}{\sigma_{\text{NLO}}}$
		LO	NLO		
$\sigma_{\text{std}}$	1.49	7.34	10.95	1.49	1.14

For the numerical results we use the following set of input parameters:  $M_W = 80.419$  GeV,  $M_Z = 91.188$  GeV,  $G_F = 1.16639 \cdot 10^{-5}$  GeV<sup>-2</sup>,  $\Gamma_Z = 2.44$  GeV. The electromagnetic coupling is defined in the  $G_\mu$  scheme. The pp cross sections are calculated at  $\sqrt{s} = 14$  TeV employing the `CTEQ6L1` and `CTEQ6M` parton distribution functions at tree- and loop-level, for more details see [28]. Applying standard cuts:  $p_{T\ell} > 20$  GeV,  $75 \text{ GeV} < M_{\ell+\ell-} < 105$  GeV,  $|\eta_\ell| < 2.5$ ,  $75$  GeV, we find that the gluon contribution accounts for 14% to the total  $pp \rightarrow ZZ$  process.

<sup>2</sup>`GOLEM`=General One-Loop Evaluator for Matrix elements.

The  $q\bar{q}$  contribution was evaluated using MCFM [29].

The effect of the photon contribution can be seen best in the invariant mass distribution of the 4 leptons in Fig 1. Between the one- and two-Z

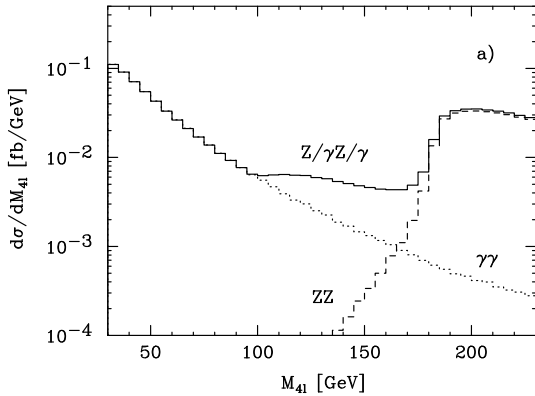


Figure 1. The invariant mass distribution of the 4 leptons including photonic contributions. Only a minimal cut  $M_{\ell^+\ell^-} > 5$  GeV is applied.

threshold the interference effects are sizable.

### 3.2. The process $PP \rightarrow ZZ + \text{jet}$

This process is of relevance in the context of Higgs searches in the Higgs plus jet channel. We have obtained analytic expressions for all 36 partonic one-loop helicity amplitudes  $q\bar{q}ZZg \rightarrow 0$  which contribute to this process. The colour structure is simple, one finds three different colour structures. By applying projection operators to each Feynman diagram, reducible scalar products between the loop momentum and external momenta can be expressed by inverse propagators and cancelled. In this way only rank one five-point functions remain, together with two-, three- and four-point tensor integrals. We use the 'tHooft-Veltman scheme which needs an accompanying prescription for  $\gamma_5$ . By splitting the  $\gamma$ -algebra and the loop momentum in a 4- and (n-4)-dimensional part we have to add a finite counterterm  $\sim (1 - \alpha_s C_F/\pi)$  to the axial coupling to

guarantee that the axial and vector part of the vector boson renormalise in the same way [30]. After UV renormalization, only IR poles remain. A finite expression can be obtained by adding the Catani-Seymour insertion operator,  $I(\epsilon)$  [2], to the result. We have integrated the resulting expression for the LHC energy over the phase space using the cut  $p_{T\text{jet}} > 100$  GeV and find:

$$\begin{aligned}\sigma_{LO} &= 1003.1 \pm 0.4 \text{ fb} \\ \sigma_{LO+virt.} &= 899.0 \pm 4.7 \text{ fb}\end{aligned}$$

Here  $M_W = 80.403$  GeV,  $M_Z = 91.1876$  GeV,  $G_F = 1.16637 \cdot 10^{-5}$  GeV $^{-2}$  are used.  $\alpha$  is evaluated in the  $G_\mu$  scheme and we used  $\mu_R = \mu_F = M_Z$ . For the LO result we use the CTEQ6L1 and for NLO the CTEQ6M parton distribution functions.  $\alpha_s$  is evaluated using the LHAPDF routines. Note that the number does not include the closed fermion loop contribution to this process as it turned out to be numerically irrelevant.

We compare the scale dependence of the LO term and the NLO virtual part in Fig 2. The figures indicate that the inclusion of the virtual corrections indeed stabilise the prediction for scales around  $2M_Z$ . Note that the real emission part of the NLO correction will add another  $\mu_F$  dependent term which stems from the initial state singularities. As new colour channels are present at NLO one expects actually a deterioration of the scale dependence, as has been observed in the  $PP \rightarrow W^+W^- + \text{jet}$  case [31].

Results for this related process have been presented by two other groups already [31,32]. We have also evaluated this process and compared our evaluation with both groups for single phase space points. Perfect agreement was found [1].

### 3.3. The process $u\bar{u} \rightarrow s\bar{s}b\bar{b}$

Signatures of beyond SM processes contain typically leptons, jets and missing energy and one easily reaches large numbers of final state partons at the LHC. Up to now no complete 6-point process, which is related to a  $2 \rightarrow 4$  kinematics, is evaluated at next-to-leading order in  $\alpha_s$ . Note that progress in that direction has been reported for the process  $pp \rightarrow b\bar{b}t\bar{t}$  at this workshop [33,34]. An example for another relevant 6-point process emerges in two Higgs doublet models, which lead

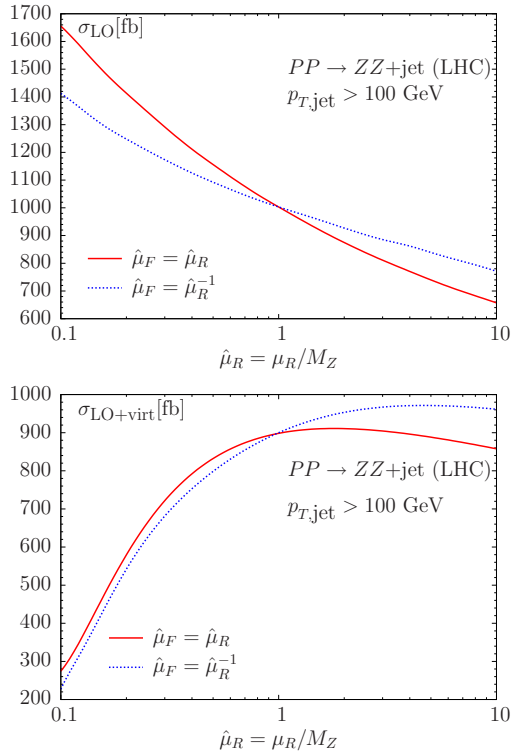


Figure 2. Scale dependence of the LO and virtual next-to-leading order corrections. The two curves in each plot show diagonal and anti-diagonal variation of the scales.

in certain parameter regions predominantly to 4 b-jets in the final state. To understand the related background in detail, the process  $PP \rightarrow b\bar{b}b\bar{b}$  has to be known at NLO. Note that at the LHC one can safely neglect the bottom mass, if realistic  $p_T$  and  $b$  separation cuts are applied. The partonic amplitudes  $u\bar{u} \rightarrow s\bar{s}b\bar{b}$  and  $g\bar{g} \rightarrow s\bar{s}b\bar{b}$  are sufficient to predict this cross section in the massless limit. We report here on the successful evaluation of the virtual part of the first of these two amplitudes.

In detail, the  $u\bar{u} \rightarrow s\bar{s}b\bar{b}$  amplitude can be written in terms of six colour structures. Two independent helicity amplitudes,  $\mathcal{A}^{++++++}$  and  $\mathcal{A}^{++++--}$ , are needed. They were evaluated in

two completely independent ways. In one evaluation a fully symbolic reduction to scalar integrals was performed, in the other one each Feynman diagram was mapped to a form factor representation and translated into a FORTRAN90 code. Both calculations are highly automated such that the evaluation of other processes only needs the respective Feynman diagrammatic input and the specification of colour and helicity projections. In the given case one has to evaluate 25 pentagon and 8 hexagon diagrams. After UV renormalization and adding the IR insertion operator all poles in  $1/(n-4)$  cancel and one is left with a finite expression which can be evaluated numerically. The FORTRAN90 code was organized such that the reevaluation of algebraic terms was avoided by recursive organization of the expressions and caching. The evaluation time for one phase space point of the full amplitude, summed over helicities and colour is about 0.8 seconds on a 3.2 GHz Intel Pentium 4 processor. As the integration over phase space can be trivially parallelised this is sufficiently fast in what concerns the evaluation of distributions.

As the evaluation of the amplitude needs a large number of numerical operations, one typically observes numerical problems in parts of the phase space where denominators become small and form factors, respectively scalar integrals, are not linearly independent anymore. If one integrates directly the LO plus finite virtual corrections over the phase space, adaptive numerical integrators tend to sample phase space points in these critical phase space regions. This happens if the induced variations influence the result at the order of the accuracy goal. To avoid this kind of destabilisation we have applied the following method for integrating the virtual NLO corrections.

We first evaluate the LO contribution over the target phase space

$$\sigma_{LO} = \int d\vec{x} f_0(\vec{x})$$

and generate unweighted events  $E_{j=1,\dots,N}$ . The latter are related to a parameter transformation  $\vec{x} \rightarrow \vec{y}$  on phase space such that the new variables have constant density  $d\vec{y} \sim d\vec{x} f_0(\vec{x}) / \sigma_{LO}$ . Any

observable  $\mathcal{O}$  can be estimated by distributing the unweighted events,  $E_j$ , into the respective bins.

$$\langle \mathcal{O} \rangle_{LO} = \frac{\sigma_{LO}}{N} \sum_{j=1}^N \chi(E_j), \quad \chi(E_j) = \begin{cases} 1, & E_j \in \mathcal{O} \\ 0, & \text{else} \end{cases}$$

An estimate of the LO plus virtual corrections can now be obtained using the same set of events. The relation

$$\sigma_{LO+virtual} = \int d\vec{x} f_1(\vec{x}) = \sigma_{LO} \int d\vec{y} K(\vec{y}),$$

where  $K = f_1/f_0$  is a local K-factor, implies

$$\langle \mathcal{O} \rangle_{LO+virt.} = \frac{\sigma_{LO}}{N} \sum_{j=1}^N \chi(E_j) K(E_j),$$

which is a simple reweighting of a LO event sample. For this purpose the LO events should be evaluated with NLO pdfs. In this way no integration over the finite virtual corrections is needed, one simply has to evaluate the virtual corrections for each unweighted event which belongs to a specified observable. Of course it still can happen that this evaluation is plagued by numerical problems but it does not negatively affect the sampling of test points in integration methods. This method leads to a good estimate if the virtual corrections are sufficiently close to the LO distribution, such that the unweighted events are also representative for the LO+virtual differential cross section. Note that this has to be fulfilled for any observable for which perturbation theory is meaningful in the first place.

To illustrate this method we show in Fig. 3 the effect of the virtual contribution on the distribution of the leading jet, i.e. the jet with the highest energy. To define the LO 4-jet observable we use the cuts:  $p_{Tj} > 50$  GeV,  $|\eta_j| < 3$  and  $\Delta R = \sqrt{\Delta\phi^2 + \Delta\eta^2} > 0.3$ . The LO cross section and the corresponding unweighted events were evaluated using WHIZARD [35] with CTEQ6M pdfs and the scale choice  $\sum_{j=1}^4 p_{Tj}/4$ ,  $\mu = 100$  GeV and one-loop running for  $\alpha_s$ . The LO + finite virtual contribution was evaluated as described above. For the LO and LO+virtual contribution we obtain

$$\begin{aligned} \sigma_{LO} &= 88.5 \pm 0.2 \text{ fb} \\ \sigma_{LO+virtual} &= 69.0 \pm 0.2 \text{ fb} \end{aligned}$$

The histograms in Fig. 3 are filled with 200,000

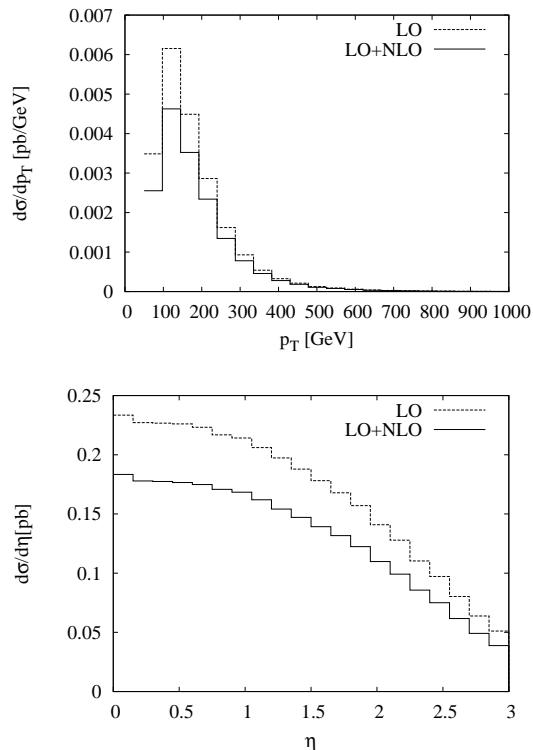


Figure 3. The  $p_T$  and rapidity distribution of the leading jet. The full line is the LO, the dashed line is obtained by adding the UV/IR finite contribution of the virtual part of the NLO prediction, as defined in the text.

unweighted events. When evaluating the local K-factors, less than 1% of all points showed an indication of numerical instability. These critical points were simply reevaluated by using the quadruple precision version of our code. A similar evaluation of the  $gg \rightarrow s\bar{s}b\bar{b}$  amplitude and the combination with the real emission corrections is in progress.

#### 4. Conclusion

In this talk we have presented recent results of the GOLEM collaboration. The implementation of our method to evaluate Feynman diagrammatic representations of amplitudes in symbolic/numerical computer programs has been completed in the context of one-loop amplitude evaluations relevant for the LHC. Here we presented results for the process  $gg \rightarrow Z^*Z^*$ , and the virtual corrections to  $PP \rightarrow ZZj$  and  $u\bar{u} \rightarrow s\bar{s}b\bar{b}$ . We have proposed a new indirect integration method for virtual corrections which is based on the evaluation of local K-factors for unweighted events defined by the LO cross section. We conclude that our method is numerically efficient and can provide predictions for multi-leg one loop processes at TeV colliders.

#### REFERENCES

1. Z. Bern *et al.* [NLO Multileg Working Group], 0803.0494 [hep-ph].
2. S. Catani and M. H. Seymour, Nucl. Phys. B **485**, 291 (1997) [Erratum-ibid. B **510**, 503 (1998)] [hep-ph/9605323].
3. T. Gleisberg and F. Krauss, Eur. Phys. J. C **53**, 501 (2008) [0709.2881 [hep-ph]].
4. M. H. Seymour and C. Tevlin, 0803.2231 [hep-ph].
5. C. F. Berger *et al.*, 0803.4180 [hep-ph].
6. S. Catani, T. Gleisberg, F. Krauss, G. Rodrigo and J. C. Winter, 0804.3170 [hep-ph].
7. W. T. Giele and G. Zanderighi, 0805.2152 [hep-ph].
8. R. K. Ellis, W. T. Giele, Z. Kunszt and K. Melnikov, 0806.3467 [hep-ph].
9. R. Britto, B. Feng and P. Mastrolia, 0803.1989 [hep-ph].
10. G. Ossola, C. G. Papadopoulos and R. Pittau, Nucl. Phys. B **763** (2007) 147 [hep-ph/0609007].
11. A. Denner and S. Dittmaier, Nucl. Phys. B **734** (2006) 62 [hep-ph/0509141].
12. Z. Bern, L. J. Dixon and D. A. Kosower, Annals Phys. **322** (2007) 1587 [0704.2798 [hep-ph]].
13. T. Binoth, J. P. Guillet, G. Heinrich, E. Pilion and C. Schubert, JHEP **0510** (2005) 015 [hep-ph/0504267].
14. T. Binoth, J. P. Guillet and G. Heinrich, Nucl. Phys. B **572** (2000) 361 [hep-ph/9911342].
15. P. Nogueira, J. Comput. Phys. **105**, 279 (1993).
16. J. A. M. Vermaseren, math-ph/0010025; see also these proceedings.
17. T. Hahn and M. Perez-Victoria, Comput. Phys. Commun. **118**, 153 (1999) [hep-ph/9807565].
18. T. Binoth, J. P. Guillet and G. Heinrich, JHEP **0702**, 013 (2007) [hep-ph/0609054].
19. T. Binoth, S. Karg, N. Kauer and R. Ruckl, Phys. Rev. D **74** (2006) 113008 [hep-ph/0608057].
20. J. R. Andersen, T. Binoth, G. Heinrich and J. M. Smillie, 0709.3513 [hep-ph].
21. T. Binoth, G. Heinrich, T. Gehrmann and P. Mastrolia, Phys. Lett. B **649** (2007) 422 [hep-ph/0703311].
22. C. Bernicot and J. P. Guillet, JHEP **0801** (2008) 059 [0711.4713 [hep-ph]].
23. T. Binoth, M. Ciccolini, N. Kauer and M. Kramer, JHEP **0612**, 046 (2006) [hep-ph/0611170].
24. T. Binoth, M. Ciccolini, N. Kauer and M. Kramer, JHEP **0503**, 065 (2005) [hep-ph/0503094].
25. M. Dührssen, K. Jakobs, J. J. van der Bij and P. Marquard, JHEP **0505** (2005) 064 [arXiv:hep-ph/0504006].
26. C. Zecher, T. Matsuura and J. J. van der Bij, Z. Phys. C **64**, 219 (1994) [hep-ph/9404295].
27. The code can be downloaded from <http://hepsource.sf.net/programs/>.
28. N. E. Adam *et al.*, 0803.1154 [hep-ph].
29. J. M. Campbell and R. K. Ellis, Phys. Rev. D **62** (2000) 114012 [hep-ph/0006304].
30. S. A. Larin, Phys. Lett. B **303**, 113 (1993) [hep-ph/9302240].
31. S. Dittmaier, S. Kallweit and P. Uwer, 0710.1577 [hep-ph].
32. J. M. Campbell, R. K. Ellis and G. Zanderighi, 0710.1832 [hep-ph].
33. A. Bredenstein, A. Denner, S. Dittmaier and S. Pozzorini, 0807.1453 [hep-ph].

34. A. Bredenstein, A. Denner, S. Dittmaier and S. Pozzorini, 0807.1248 [hep-ph].
35. W. Kilian, T. Ohl and J. Reuter, 0708.4233 [hep-ph].